EPJ manuscript No.
(will be inserted by the editor)

Lattice QCD and Neutrino-Nucleus Scattering

Andreas S. Kronfeld[1a], David G. Richards[2b], William Detmold[3], Rajan Gupta[4], Huey-Wen Lin[5], Keh-Fei Liu[6], Aaron S. Meyer[7], Raza Sufian[2], and Sergey Syritsyn[8]

[1] Theoretical Physics Department, Fermi National Accelerator Laboratory, Batavia, IL 60510, USA
[2] Theory Center, Thomas Jefferson National Accelerator Facility, Newport News, VA 23606, USA
[3] Center for Theoretical Physics, Massachusetts Institute of Technology, Cambridge, MA 02139, USA
[4] Group T-2, Los Alamos National Laboratory, Los Alamos, NM 87545, USA
[5] Department of Physics and Astronomy, Michigan State University, East Lansing, MI 48824, USA
[6] Department of Physics and Astronomy, University of Kentucky, Lexington, KY 40508, USA
[7] Physics Department, Brookhaven National Laboratory, Upton, NY 11973, USA
[8] Department of Physics and Astronomy, Stony Brook University, Stony Brook, NY 11794, USA

the date of receipt and acceptance should be inserted later

Abstract. This document is one of a series of whitepapers from the USQCD collaboration. Here, we discuss opportunities for lattice QCD in neutrino-oscillation physics, which inevitably entails nucleon and nuclear structure. In addition to discussing pertinent lattice-QCD calculations of nucleon and nuclear matrix elements, the interplay with models of nuclei is discussed. This program of lattice-QCD calculations is relevant to current and upcoming neutrino experiments, becoming increasingly important on the timescale of LBNF/DUNE and HyperK.

Executive Summary

In 2018, the USQCD collaboration's Executive Committee organized several subcommittees to recognize future opportunities and formulate possible goals for lattice field theory calculations in several physics areas. The conclusions of these studies, along with community input, are presented in seven whitepapers [1,2,3,4,5,6]. This whitepaper covers the role of lattice QCD in neutrino-nucleus scattering, motivated principally by neutrino oscillations.

Neutrino-nucleus scattering experiments provide a wealth of information on neutrino masses and flavor mixing, on nucleon and nuclear structure, and on non-standard interactions between neutrinos and ordinary matter. To interpret these experiments cleanly, the key problem is to reconstruct the incident neutrino energy. The nuclear remnant is not, in these experiments, detected. It is therefore impossible to reconstruct the neutrino energy without modeling the nucleus in some way. This problem is complex, because it spans a range of energies—from hundreds of keV to a few GeV—that probe all aspects of the target nucleus.

The presence of many energy scales implies that a variety of theoretical techniques must work in concert. A convenient, organizational framework is nuclear many-body theory, which takes nucleonic properties as inputs. In this whitepaper, we discuss how these nucleonic properties can be obtained directly from the QCD Lagrangian using numerical simulations of lattice gauge theory. Although lattice QCD cannot settle every question in neutrino-nucleus scattering, it is reasonable to demand that our understanding of these processes be consistent with QCD. In many cases, the most straightforward route to the needed QCD knowledge is lattice QCD.

In this whitepaper, we discuss several calculations that should, as they mature, be incorporated into nuclear theory and neutrino event generators. A very important and very feasible example is the axial form factor of the nucleon. Lattice QCD has a notable history of calculating this and related observables, and calculations with full control of the systematic uncertainties are now coming of age. Here, "full control of systematic uncertainties" implies that a complete error budget is provided. The axial form factor is relatively straightforward: completely analogous calculations of vector form factors are possible with the same (indeed, overlapping) computational effort. The vector form factors have been measured in electron-proton and -neutron scattering, so an apt crosscheck is close at hand. Experience from form factors in meson physics suggests a simple, model-independent way to transmit the output of lattice QCD to event generators and, thus, analysis of experimental data.

Form factors of nucleons are only the beginning. Future oscillation experiments span beam energies such that computationally more demanding information is required. Just at the nucleon level, transition form factors to multibody final states are needed. For an inclusive data set,

[a] *email:* ask@fnal.gov
[b] *email:* dgr@jlab.org

the object of interest is the nuclear hadron tensor, which can be obtained by combining the nucleonic hadron tensor from lattice QCD with a nuclear spectral function. In the deep inelastic region, new ways of computing parton distribution functions in lattice QCD are an exciting development. A further emerging component of lattice QCD consists of calculations of the properties of small nuclei—up to ^{4}He today and to ^{6}Li with exascale computing—can be used to test nuclear many-body theory and provide information via chiral effective theories to pin down the nuclear physics.

Lattice-QCD calculations with nucleon and nuclei are more challenging than the corresponding ones for mesons, because of unavoidable technical challenges that increase with the number of quark lines. Consequently, to perform the requisite calculations, improvements in methodology, algorithms, and software will be essential. Even assuming continuing ingenuity on those fronts, much of the work will require exascale computing resources. As in the past, a combination of high-capability and high-capacity computing will be needed. The former is needed for timely solution of mature problems, while the latter is necessary for developing feasible techniques for the challenging calculations, before making the jump to supercomputer centers.

1 Introduction

Along with the first observation of the Higgs boson and the mounting evidence for dark matter, the discovery that neutrinos change flavor is one of the major advances in particle physics over the past twenty-five years. The discovery hinged on studies of neutrinos produced at the upper edge of the earth's atmosphere [7] and also explained a deficit in electron neutrinos from the sun [8]. These findings prompted an accelerator-based experimental program in Europe, Japan, and the United States, to make more accurate measurements of, for example, the squared mass differences. The increase in precision and sensitivity expected in future experiments raises the question whether the theoretical description of the relevant experiments must be further refined to exploit the new measurements to the fullest. In particular, as future, ambitious, long-baseline neutrino-oscillation experiments such as LBNF/DUNE [9] and HyperK [10] have come into focus, the quantification of uncertainties from the hadronic and nuclear physics of the detectors have become increasingly relevant. To this end, the lattice-QCD community has identified a set of feasible calculations that will be of special relevance. This program is described in this whitepaper.

An important goal of the experimental neutrino-physics program is to test the three-neutrino paradigm of the Standard Model. In this context, the Standard Model must be extended to allow for lepton flavor change. The simplest choice consistent with the standard gauge symmetries is to introduce a set of right-handed neutrino fields. Then lepton-flavor mixing and neutrino masses arise in the same way as in the quark sector, namely through Yukawa couplings to the Higgs field with a nonvanishing vacuum expectation value. To couple to the Higgs and left-handed-lepton doublets, the right-handed neutrino fields have to be gauge singlets. But then no symmetry principle forbids a mass term connecting neutrinos to themselves (i.e., of the kind first noted by Majorana [11]), in contrast to the Higgs-generated Dirac mass term, which connects neutrino to antineutrino. The lack of direct evidence for right-handed neutrinos suggests that in this scenario the Majorana mass M might be very large. If one supposes that the neutrino Yukawa couplings are not much different from light quarks or charged leptons, the propagating neutrinos have mass close to M and to $m_\nu \approx y^2v^2/2M$, where y is a Yukawa coupling and v is the vacuum expectation value of the Higgs field. This mass hierarchy, known as the see-saw mechanism, provides a possible explanation of the tiny size of neutrino masses [12,13,14]. For example, if M is a grand-unified mass scale around 10^{15} GeV, then $m_\nu \lesssim 0.03$ eV (for $y \lesssim 1$).

This theoretical framework means that the three-neutrino paradigm can be tested by measuring the neutrino mass-squared differences and the mixing angles and CP violating phases of the Pontecorvo-Maki-Nakagawa-Sakata (PMNS) mixing matrix [15,16,17]. As in the case of the Cabibbo-Kobayashi-Maskawa (CKM) quark-mixing matrix [18,19], the PMNS has three mixing angles. If the Majorana mass term appears, the PMNS matrix has three CP-violating phases instead of one as in the CKM matrix. The mixing angles and the CKM-like CP-violating phase can be measured in oscillation experiments, while the extra phases and the Majorana nature of neutrinos can be probed via the neutrinoless double-beta ($0\nu\beta\beta$) decay of certain nuclei. For lattice-QCD calculations relevant to $0\nu\beta\beta$, see the companion whitepaper "The Role of Lattice QCD in Searches for Violations of Fundamental Symmetries and Signals for New Physics" [3]; here, the focus is on lattice-QCD research that will impact the oscillation experiments.

Oscillation experiments measure the energy spectrum of a neutrino beam after it has travelled a certain baseline distance. Unfortunately, neutrino beams have a wide energy spectrum, as shown in Fig. 1, so the center-of-mass energy of a collision is not known. In contrast, quark-flavor experiments, for which lattice QCD has been crucial, study decays of strange, charmed, or b-flavored hadrons of precisely known mass. Here, the energy of the incident neutrino must be inferred from measurements of the final state. The targets in neutrino experiments are medium- to large-sized nuclei, such as ^{12}C, ^{16}O, or ^{40}Ar, the remnants of which are not, in practice, be detected. That means that the mapping between final-state measurements and the initial energy inevitably requires theoretical knowledge of the neutrino interaction with the struck nucleus.

Consistency with QCD is a clearly desirable characteristic of nuclear models used to deduce the connection between final and initial states. Thus, it makes sense to incorporate lattice QCD as soon as results with full, reliable error budgets are available. As discussed in more detail in Ref. [21], the nuclear models rely in part on properties of the nucleon as inputs. Many of these quantities can be

calculated in lattice QCD in the near term, with the precision depending on the quantity. Of course, single-nucleon calculations are not in themselves enough. Calculations of the properties of multi-nucleon systems must be developed concurrently and, once mature, also incorporated into the nuclear modeling.

The theory behind neutrino-nucleus collisions is complex because it spans a range of energies that probe all aspects of the target nucleus. Nuclear excitation energies are, typically, dozens of keV, while the average binding energy is 8.6 MeV (in ^{40}Ar), and the typical Fermi motion of a nucleon is around 250 MeV. In the regime relevant to oscillation experiments, the energy transfer to the nucleus ranges between ∼200 MeV and the neutrino energy itself, although much of transferred energy is carried off by nucleons and pions, rather than the nuclear remnant. Thus, it is a challenge to arrive at a comprehensive approach to the entire problem. Most approaches start with nuclear many-body theories, in which the nucleus is described by a nuclear wave function of a collection of interacting nucleons; see, for example, Ref. [22,23]. It is at this point in the analysis that nucleon-level matrix elements enter. One should bear in mind, however, that single-nucleon physics is not enough: multi-body effects are needed for scattering events that knock out two (or more) nucleons. Even in nuclear spectroscopy, three-body potentials improve the agreement with observed nuclear levels [24,25,23]. Often these calculations use phenomenological potentials, but effective field theory (EFT) offers a direct connection to QCD [26,27,28,29]. Chiral EFTs are, however, limited to a kinematic range where the momenta are small relative to the chiral symmetry breaking scale $\Lambda_\chi \sim 700$ MeV. Even then, the reliability of the application of nuclear EFT to large atomic number systems, such as argon, requires significant development, testing, and, eventually, verification. These issues are further intertwined with the constraints of how event generators [30,32,36,33,35] and detector simulations are implemented. Inconsistencies arise in the current approach where, for example, the axial form factor of the nucleon is extracted from νA scattering data assuming one nuclear model and then used in event generators employing another.

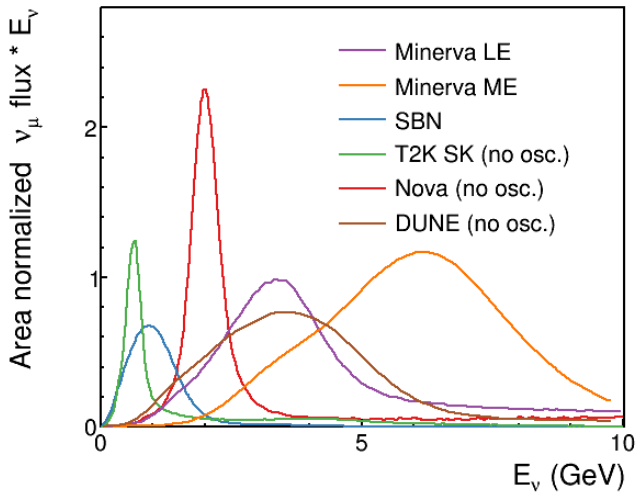

Fig. 1. Energy spectrum of the neutrino beam for several experiments. In particular, most of DUNE's beam lies in the range 1 GeV $< E_\mu <$ 7 GeV. Courtesy Laura Fields [20].

A central goal of nuclear theory in this arena should therefore be to define a path forward that allows for a quantified nuclear uncertainty to be presented for experiments such as DUNE and HyperK. Achieving this is a challenging task and will require input and constraints from lattice QCD in order for it to be successful. In addition to the single- and few-nucleon amplitudes noted above, it will be valuable to compute directly the properties of small nuclei. At present, calculations involving nuclei up to ^{4}He are possible. In addition to being interesting in their own right, such lattice-QCD calculations of few nucleon systems can be used to constrain low energy constants (LECs) in the EFTs. This approach has already been applied to static quantities, such as magnetic moments. A next step will be to work with matrix elements of electroweak currents, to build up effects associated with two- and higher-body contributions, as well as more complex contributions such as pion production. In combination with experimental constraints from eA scattering, and neutrino scattering on light nuclear targets,[1] it is hoped a robust uncertainty can be determined.

To study neutrino oscillations, we are interested in the processes

$$\nu_\ell A \to \ell^- X, \qquad \bar\nu_\ell A \to \ell^+ X, \tag{1}$$

where A denotes the nucleus and X the combination of all final-state hadrons including the remnant of the nucleus. The charged weak current responsible for these interactions has the well-known $V-A$ structure. Properties of the vector current can be inferred from electromagnetic scattering, up to isospin corrections (which are negligible for the needed precision; see Sec. 4). On the other hand, because the weak charge of the proton is so small, $Q_{\rm w}^p = 0.0719 \pm 0.0045$ [38], at the energies of interest, only neutron-neutrino (and proton-antineutrino) scattering is sensitive to the axial current. These circumstances offer the possibility of testing lattice-QCD methodology with the vector current before relying on it for the axial current.

The quantity needed to describe the strong-interaction side of the scattering depends on the energy transferred. At the lowest energies, the only possibility is coherent elastic scattering via the weak neutral current, with $X = A$ [39,40]. Coherent neutrino-nucleus interactions have recently been observed for the first time [41]. As the energy increases slightly, the excitation spectrum of A is traced out: $X = A^*$. The needed quantities are matrix elements between different nuclear levels. In lattice QCD, one would have to simulate the whole nucleus directly, which is currently feasible only for nuclei much smaller than those in the cesium-iodide detector of Ref. [41].

[1] Indeed, recent discussions of future experiments with deuterium or hydrogen targets [37] hinge on noting the utility of nucleon-level amplitudes in nuclear many-body theory.

At high enough (but still low) energy, a single nucleon can be knocked out. At its heart, the scattering is

$$\nu_\ell n \to l^- p, \qquad \bar{\nu}_\ell p \to l^+ n, \tag{2}$$

with the initial and final-state nucleons in the nuclear environment. Such scattering off of a constituent in a bound-state without extra particles is known as quasielastic. Then nuclear many-body theory requires single-nucleon matrix elements of the form $\langle p(p')|J_\nu|n(p)\rangle$, between a neutron of momentum p and a proton of momentum p' (or the $p \to n$ counterpart for antineutrino beams). These matrix elements are straightforward to calculate in lattice QCD; see Sec. 2. If pions can be produced, the final state can be a $\Delta(1232)$ resonance, an excited nucleon N^*, or a two-body state $N\pi$. In the experiment, these all end up as $N\pi$ so their amplitudes interfere. In fact, lattice QCD can provide not only the associated transition matrix elements, in the idealization of the resonance as a stable particle (e.g., $\langle\Delta^+|J_\nu|n\rangle$), but also enough information to describe the full multi-hadron nature of the final state (at least up to further inelasticities); see Sec. 3. The quasielastic and resonance regions overlap, because the kinetic energy of Fermi motion is a bit larger than the pion mass. This overlap is illustrated with experimental data in Fig. 2. Another contribution in this region arises from many-body nuclear dynamics, for example, when the probe interacts with pairs of correlated nucleons. This contribution is described by "two-body currents" (see Refs. [43,44] and references therein). Now a further set of matrix elements is needed, namely of the form $\langle NN|J_\nu|NN\rangle$. This contribution is significant because of correlated pairs in the nuclear wave function and is often referred to the two-particle–two-hole (2p-2h) contribution [45,46,47,48,49]. Note that in QCD language, the same current is employed; the two-body nature is in the initial and final states.

Once the energy is high enough to produce several pions, it is not possible to enumerate every final-state hadron. In this case, however, lattice QCD can be used to compute nucleon and nuclear structure functions. In high-energy physics, structure functions are most familiar in deep-inelastic scattering, where the operator-product expansion (OPE) can be used. Lattice-QCD calculations can be used to determine the moments of the parton distribution functions (PDFs) that enter in the deep-inelastic region, and indeed extraction of the full dependence of PDFs on the longitudinal momentum fraction, x, is becoming possible [50]. Moreover, the definition of structure functions is very general. Lattice QCD may be an ideal way to compute them in the so-called shallow-inelastic region with energy above the resonance region but insufficient for the OPE; see Sec. 3.

In summary, then, the goals for lattice QCD for neutrino oscillation physics are to calculate matrix elements of the form

$$\langle f|J_\nu|i\rangle, \qquad \langle f|J_\mu^\dagger J_\nu|i\rangle, \qquad \langle f|\mathcal{O}|i\rangle, \tag{3}$$

where the initial and final states are single nucleons, two nucleons, nucleons with a pion (including resonances), or small nuclei. In the last case, $\mathcal{O}$ denotes an operator appearing in the OPE, or a bilocal, spatially-separated operator arising in the calculation of PDFs. The lattice-QCD calculations of these and related matrix elements have a long history, motivated principally by the desire to understand nucleon and nuclear structure. For a broad survey, see our companion whitepaper "Hadrons and Nuclei" [4].

Recall that lattice QCD calculates hadronic correlation functions, which contain information about the masses and matrix elements of interest; the information is extracted by fitting the behavior of the correlation functions in (Euclidean) time. Several technical difficulties make baryon calculations more difficult than the corresponding calculations for mesons. First, statistical errors on baryon correlation functions are larger and more poorly behaved in time [54,55,56]. Second, it has proven more difficult, in practice, to disentangle matrix elements of the ground-state baryons from that of their excitations [57, 58,59]. Last, the dependence of baryon properties on the light quark mass (used in the simulation) is less well described by the low-energy EFT of pions and baryons. All

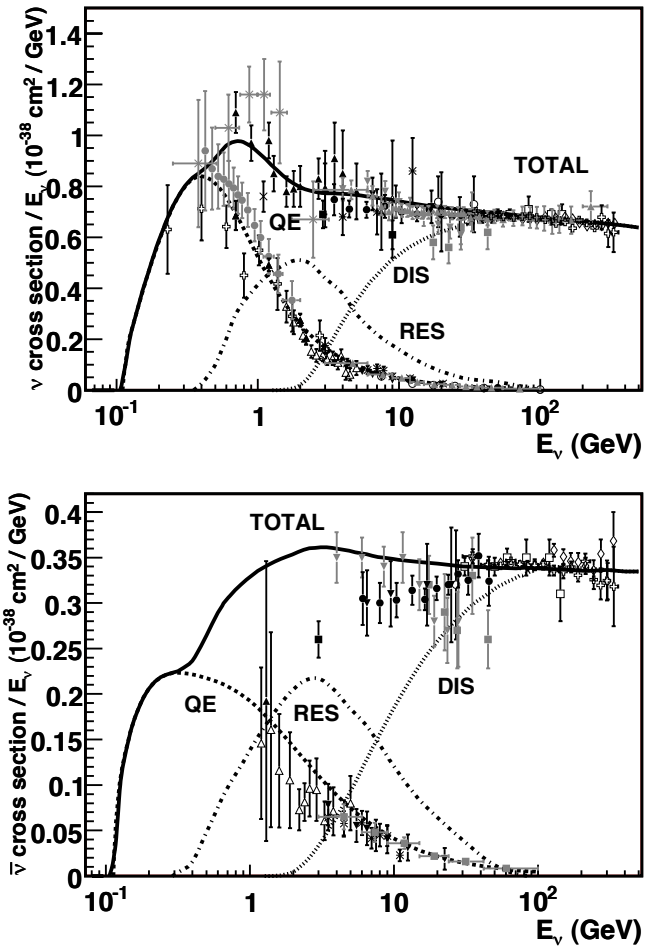

Fig. 2. Cross sections vs neutrino energy (top) or antineutrino energy (bottom), showing the relative contributions of the underlying processes quasielastic scattering, resonance production, and deep-inelastic scattering [42].

these difficulties can be addressed with more computing. The signal-to-noise problem can clearly be attacked with higher statistics. It can also be mitigated by choosing more sophisticated operators to create and annihilate baryon states; this method is also the way to better filter out the excited states. Finally, more computing also enables simulations with lighter and even physical quark masses [51, 52, 60].

The rest of this whitepaper is organized as follows. In Sec. 2, we discuss calculations that are relatively straightforward. These include nucleon form factors, which are needed to describe quasielastic scattering, and moments of PDFs, which are needed in the deep-inelastic region. We discuss the form factors in considerable detail, because the time to incorporate these results into event generators is soon or, arguably, now. In particular, having the correct slopes for the form factors is crucial to gaining quantitative control of the cross section. More challenging calculations are covered in Sec. 3. This class of problems is large and varied: transitions to resonances and multibody states, calculations for shallow- and deep-inelastic scattering, and the vector and axial matrix elements of small nuclei. Section 4 turns to calculations that are far enough beyond that state of the art that new ideas or computing facilities greater than exascale are needed. Foreseeable computing needs are covered in Sec. 5, noting the separate needs for both capability and capacity computing.

2 Straightforward calculations

The most straightforward matrix elements to calculate are those with one stable hadron in the initial state, and one or none in the final state. Here we focus on the matrix elements of electroweak currents, $\langle N|J_\mu|N\rangle$, which directly enter neutrino-nucleon scattering, and matrix elements of local operators, $\langle N|\mathcal{O}|N\rangle$, where $\mathcal{O}$ appears in the operator-product expansion of two J currents, which arise in the analysis of deep-inelastic scattering.

2.1 Nucleon form factors

As discussed in Sec. 1, neutrino-nucleon scattering, Eq. (2) is a key process even though the target is a nucleus. The $V-A$ charged current of interest is $J^+_\mu = \bar{u}\gamma_\mu(1-\gamma_5)d$. The matrix element for $n \to p$ can be decomposed into Lorentz covariant combinations of momentum and spin, multiplied by form factors [61]:

$$\begin{aligned}\langle p(p') \mid J^+_\mu \mid n(p)\rangle = \bar{u}^{(p)}(p') \Big[&\gamma_\mu F_1^{\rm CC}(q^2) + \\ &i\sigma_{\mu\nu}\frac{q^\nu}{2M_N}F_2^{\rm CC}(q^2) + \frac{q_\mu}{M_N}F_S^{\rm CC}(q^2) + \\ &\gamma_\mu\gamma_5 F_A^{\rm CC}(q^2) + \gamma_5\frac{q_\mu}{M_N}F_P^{\rm CC}(q^2) + \\ &\gamma_5\frac{(p'+p)_\mu}{M_N}F_T^{\rm CC}(q^2)\Big] u^{(n)}(p),\end{aligned} \tag{4}$$

where $M_N = (M_p + M_n)/2$, $q = p' - p$ and $\bar{u}$ and u are associated spinor factors. $F_1^{\rm CC}(q^2)$, $F_2^{\rm CC}(q^2)$, $F_A^{\rm CC}(q^2)$, and $F_P^{\rm CC}(q^2)$ are known as the Dirac, Pauli, axial, and induced pseudoscalar form factors, respectively. The induced scalar and tensor form factors, $F_S^{\rm CC}(q^2)$ and $F_T^{\rm CC}(q^2)$, are suppressed by G parity violation; they are known as second-class currents [62]. For neutral-current processes, additional form factors $F_i^{{\rm EM},N}$ and $F_i^{{\rm NC},N}$ are needed: the charged-currents are all isovector, but the neutral currents contain an isoscalar contribution as well. Here, N denotes either a proton p or neutron n.

Because the up- and down-quark masses are so similar, isospin violation can be neglected and, thus, the charged-current form factors of the vector current (i.e., Dirac and Pauli) can be related to their electromagnetic counterparts, up to small corrections from isospin violation. The Dirac and Pauli form factors are usually re-expressed as electric, $G_E(q^2) = F_1(q^2) + q^2F_2(q^2)/(M_n + M_p)^2$, and magnetic, $G_M(q^2) = F_1(q^2) + F_2(q^2)$, form factors (even for CC and NC). Expressions relating the differential neutrino-nucleon cross section to the form factors can be found, for example, in Refs. [63, 42].

Most neutrino scattering experiments are performed in a kinematic region of a few GeV, so tracing out the full q^2 dependence is possible and desirable (see below). Below 1 GeV it is convenient to focus attention on the intercepts $F_i(0)$ and (conventionally normalized) slopes

$$\begin{aligned} r_E^2 &\equiv 6\,\frac{dG_E}{dq^2}\bigg|_{q^2=0}, \\ r_M^2 &\equiv \frac{6}{G_M(0)}\,\frac{dG_M}{dq^2}\bigg|_{q^2=0}, \\ r_i^2 &\equiv \frac{6}{F_i(0)}\,\frac{dF_i}{dq^2}\bigg|_{q^2=0}, \end{aligned} \tag{5}$$

for $i \in \{A, S, T, P\}$. The quantities r_i are usually called "radii", although the neutron's r_E^2 is negative.

A precise knowledge of the charged-current versions of these quantities is essential for determining the neutrino-nucleon cross section. The intercepts and slopes of $G_E^{\rm CC}$ and $G_M^{\rm CC}$ are well determined from electromagnetic processes and isospin relations. Further, the intercept $F_A^{\rm CC}(0) = g_A = -1.2723(23)$ is known from neutron β decay [64]. The axial coupling g_A has been calculated in lattice QCD, although it will be some time before it can be computed with comparable precision to experiment. Nevertheless, it is an extremely important benchmark, and once the lattice-QCD precision becomes competitive with experiment, the result could clear up some puzzles surrounding neutron-decay measurements (see below).

On the other hand, the axial-charge radius-squared r_A^2 is less well known. Historically, the axial form factor has been fit to the so-called "dipole" form:

$$F_A(q^2) = \frac{g_A}{(1 - q^2/m_A^2)^2}, \tag{6}$$

such that $r_A^2 = 12/m_A^2$. Experiments report this "axial mass", m_A, so a comparison of reported values illustrates the current status. It has been extracted from quasielastic scattering on deuterium targets, finding (e.g.)

$m_A = 1.02(3)$ GeV [65], and from pion electroproduction, finding $m_A = 1.08(4)$ GeV [66,67]. More recent experiments find larger values: $m_A = 1.20(12)$ GeV at K2K [68], $m_A = 1.27(15)$ GeV at MINOS [69], and even $m_A = 1.35(17)$ GeV at MiniBooNE [70], in neutrino charged-current quasielastic scattering with water, iron, and mineral-oil targets, respectively. With two-particle-two-hole corrections, however, NOMAD [71], with a Kevlar target, finds $m_A = 1.05(6)$ GeV and MINERvA [72,73], with a carbon target, finds the quasielastic cross section to be compatible with $m_A = 0.99$ GeV. Note that all of these determinations of m_A assume a nuclear model for the target material, which is not the same among the various collaborations. Moreover, nuclear modeling uncertainties typically come only from varying parameters of their choice model, not from studying comparisons among different models.

The uneasy agreement of these results can be removed by switching to a model-independent parametrization of $F_A(q^2)$ [61]. For example, a reanalysis of 1980s deuterium bubble-chamber data [74] finds $\sqrt{12/r_A^2} = 1.01(24)$ GeV. These data are chosen because the nuclear model of the deuteron is under relatively good control. The main conclusion of Ref. [74] is that introducing only one free parameter with a qualitatively acceptable but conceptually incorrect shape, as in Eq. (6), leads to gross underestimates of the uncertainty, even when the fit quality is high.

Figure 4, from Ref. [75], shows the dependency of νn quasielastic cross section on E_ν, assuming r_A^2 is known with 20% uncertainty. As one can see, this quantity affects the both the normalization and fall-off of the cross section, which are needed, respectively, to determine the mixing angle and mass difference in an oscillation. Furthermore, a

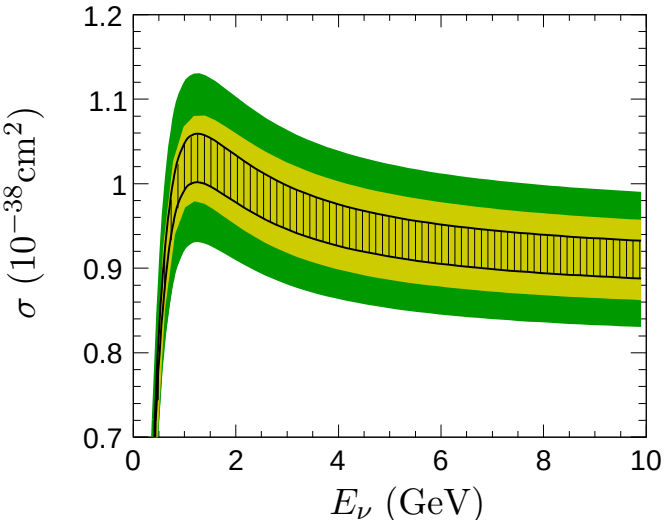

Fig. 3. Quasielastic neutrino-neutron cross section. The green band shows the uncertainty stemming from the current value of r_A^2 [74], while black hatched band shows the reduction once the uncertainty on r_A^2 is reduced to 20%. The yellow error band shows the uncertainty stemming from all other inputs. From Ref. [75].

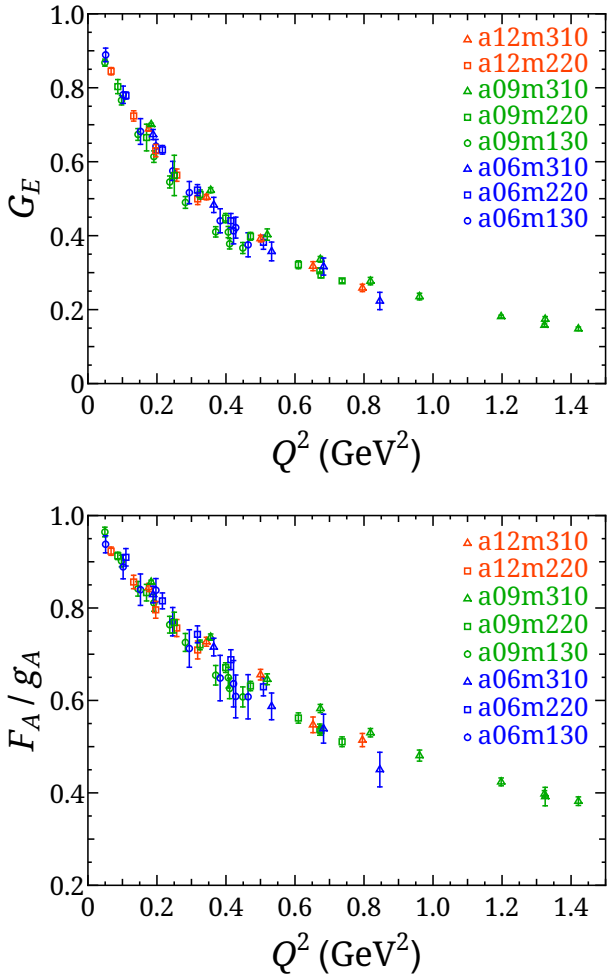

Fig. 4. Electric (top) and isovector axial (bottom) form factors of the nucleon vs $Q^2 = -q^2$. Data from Ref. [82,91].

lattice-QCD calculation with 20% uncertainty (compared to 50% in Ref. [74]) is an important milestone, because then the r_A^2 uncertainty becomes subdominant, at least until other uncertainties have been reduced.

The lattice-QCD community has been pursuing the calculation of the nucleon form factors for a long time. A representative set of recent work can be found in Refs. [76, 77,78,79,80,81,82,83,84,85,86,87,88,89,90] Significant improvements have been made to investigate the quark-mass, finite-volume, and finite-lattice-spacing dependence, and the effects of excited-state contamination in the correlation functions. With these technical and algorithmic advances, lattice QCD can calculate not only the isovector contribution but also the computationally more demanding isoscalar and strange-quark contributions, which are needed for neutral-current processes, discussed below.

Sample lattice-QCD calculations [82,91] of the nucleon isovector electric and axial form factors—G_E and F_A—are shown in Fig. 4. Eight different $2+1+1$-flavor HISQ ensembles generated by the MILC collaboration [52,53] with lattice spacings in the range 0.06–0.12 fm and pion mass in the range 130–310 MeV are employed. In this cal-

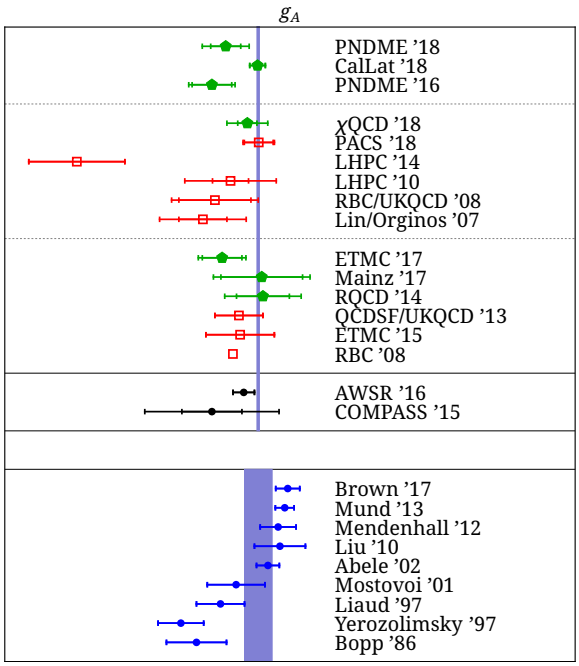

Fig. 5. Status of lattice-QCD calculations of g_A , together with non-lattice determinations, from Ref. [93]. Filled green (unfilled red) lattice-QCD results have (in)complete error budgets. The violet line in the upper panel is the PDG average of the results in the bottom panel, in which the scale is blown up by a factor of 10.

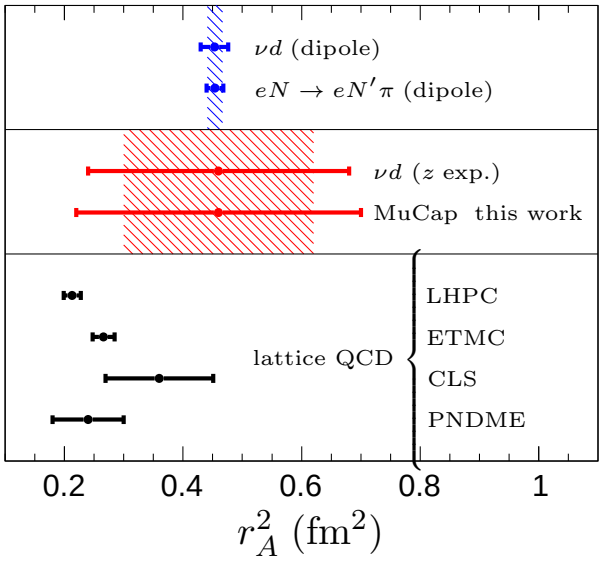

Fig. 6. Status of lattice-QCD calculations of r_A^2, together with non-lattice determinations, adapted from Ref. [75] with permission. As discussed in the text, the error bars on r_A^2 from dipole fits are underestimated and the two small lattice-QCD error bars stem from incomplete error analyses, critiqued below. The references from top to bottom are as follows: "νd and $eN \to eN'\pi$ (dipole)" [65], "νd (z exp.)" [74], "MuCap this work" [75], LHPC [78] (NB: one lattice spacing and $M_\pi = 317$ MeV), ETMC [79] (NB: no strange sea and a small volume such that $M_\pi L < 3$), CLS [80], PNDME[81].

culation, excited-state contamination is controlled via a three-state fit. The results are in good agreement with the experimental data for the nucleon electromagnetic form factor $G_E(q^2)$ On the other hand, the axial form factor is not as steep as experimental determinations with $m_A \approx 1$ GeV [92], yet is compatible with MiniBooNE's $m_A \approx 1.35$ GeV [70]. Despite the many laudable aspects of Ref. [82], a full and robust accounting of all systematics involved in these lattice-QCD calculations has not yet been feasible. Reliable confrontation with precise experimental data for G_E—and, hence, a solid prediction of F_A—requires an increase in computational resources to overcome the technical obstacles to nucleon matrix elements, discussed in Sec. 1.

The status of lattice-QCD calculations of g_A and r_A^2 is shown in Figs. 5 and 6, respectively. Fig. 5 [93] shows that lattice-QCD calculations of g_A are currently far less precise than the results from neutron β decay.[2] Note, however, that bottle and beam experiments measuring the neutron lifetime yield values of g_A that differ by 3σ. For example, a 2015 bottle measurement[98] leads to $g_A = 1.2749(11)$, while a 2013 beam measurement leads to $g_A = 1.2684(20)$ [99]. It would be interesting to know the answer from lattice QCD. The precision required depends on whether the (average of several) calculation(s) lands between the two neutron-lifetime values or outside the interval. In the latter case, at least percent-level precision is needed, which is likely to be achieved with three years (assuming sustained computing support). If lattice QCD lands in the middle, 0.3% precision is needed. In this scenario, we would also need 1+1+1(+1)-flavor ensembles, since the isospin symmetry would play an important role at such precision; it would take 5–10 years to account for full systematics.[3]

Figure 6[75], for r_A^2, shows significant problems: the analysis with the z expansion [74] debunks the uncertainty estimates of determinations predicated on the dipole form. The model independent results (red; between the horizontal lines) illustrate the best estimate of r_A^2 without such strong assumptions. One should bear in mind that the "experimental" determinations all make assumptions: without new muon capture [75] or νd and $\bar{\nu}p$ experiments [37], for which the assumptions are mild or nil, it seems nearly impossible to improve the situation via experiment. On the other hand, lattice gauge theory can provide an *ab initio* result from QCD. Indeed, lattice QCD is beginning to play a role, but another generation of calculations is needed before fully definitive results with uncertainties

[2] The color code here is adapted from the Flavor Lattice Averaging Group [94,95,96], as specified in the Appendix of Ref. [97].

[3] Note that the normalization of the matrix element can be blinded with an multiplicative offset [100], to guard against analyst bias. The results in Fig. 5 have not, however, employed this technique.

small enough to make an impact on cross section calculations are achieved.

For the full energy range of LBNF/DUNE, it will be necessary to trace out the full q^2 dependence of the form factors. It is imperative to use a model-independent parametriza-tion based on general analytic properties. In the complex-q^2 plane, the vector (axial) form factors have a cut starting at $q^2 = t_{\rm cut} \equiv 4M_\pi^2$ ($q^2 = t_{\rm cut} \equiv 9M_\pi^2$) and extending to ∞ on the real axis. The cut lies outside scattering kinematics $q^2 < 0$ but nevertheless prevents a useful series expansion in q^2 around the origin. A rigorous way to proceed is to introduce a conformal mapping that maps the cut to the unit circle [101,102]:

$$z(t) = \frac{\sqrt{t_{\rm cut} - t} - \sqrt{t_{\rm cut} - t_0}}{\sqrt{t_{\rm cut} - t} + \sqrt{t_{\rm cut} - t_0}}, \tag{7}$$

where the parameter t_0 can be chosen to center the q^2 range of interest on $z = 0$; in general, spacelike $q^2 \to -\infty$ maps to $z \to 1$. An expansion of the form

$$F(z) = \sum_k a_k z^k \tag{8}$$

thus has an expansion parameter $|z| < 1$. Moreover, unitarity in quantum mechanics ensures that the series is uniformly convergent on this interval. In fact, unitarity leads to bounds on the coefficients a_k that the dipole form, Eq. (6), violates [61].

In practice [61,103,104,105], the z expansion converges after a few terms. Because on the nonlinear mapping, even an intercept and slope in z give a form factor with a physical shape (i.e., similar to those shown in Fig. 4). As lattice data improve, more and more terms will become resolvable. As in CKM physics [104,105], lattice-QCD papers can provide the coefficients, their uncertainties, and their correlations; several lattice-QCD calculations of F_A do the same [79,80,78,81]. Finally, code for taking such z-expansion input is included in the GENIE event generator [33] module for the axial form factor, and work is underway to extend this to the vector form factor channel.

Although not crucial to neutrino oscillations, the same experiments study weak neutral-current interactions of the Z boson and, possibly, non-Standard bosons [106,107]. The corresponding Dirac and Pauli form factors can be obtained from the proton and neutron electromagnetic form factors and the strange-quark contribution (accessible in parity-violating elastic electron-scattering experiments [108]) as

$$F_i^{\rm NC} = \left(\tfrac{1}{2} - \sin^2\theta_{\rm W}\right)\left(F_i^{{\rm em},p} - F_i^{{\rm em},n}\right) - \sin^2\theta_{\rm W}\left(F_i^{{\rm em},p} + F_i^{{\rm em},n}\right) - \tfrac{1}{2}F_i^s, \tag{9}$$

where $i \in \{1,2\}$. Using the most recent z-expansion fit to nucleon electromagnetic form factors [109] and a new lattice-QCD calculation of strange-quark form factors [110], one can see that the strange-quark contribution increases the neutral-current Pauli form factor, $F_2^{\rm NC}(q^2)$, by about 3.1% and 2.5% at $q^2 = 0$ and $q^2 = -0.1$ GeV^2, respectively. Although the strange-quark contribution is small, the coefficients $(\frac{1}{2} - \sin^2\theta_{\rm W})$ and $\sin^2\theta_{\rm W}$ suppress the two combinations of nucleon electromagnetic form factors in Eq. (9), such that the strange-quark sea makes an important contribution to $F_2^{\rm NC}(q^2)$ at low q^2.

Similarly, assuming isospin symmetry and the absence of second-class currents, one can relate the neutral-current axial form factor to the charged-current axial and strange-quark axial form factors [111,112]:

$$F_A^{\rm NC} = \tfrac{1}{2}(-F_A^{\rm CC} + F_A^s). \tag{10}$$

It has been shown [113,114] that the effect of Pauli blocking becomes very significant in the region $0 < -q^2 \lesssim 0.2$ GeV^2. Therefore, a precise lattice-QCD calculation of $F_A^{\rm NC}(q^2)$ is required for a precise estimate of the neutral-current (anti)neutrino-nucleon scattering cross section.

Finally, we note that quasielastic neutrino and antineutrino scattering would be sensitive to the presence of the second-class currents, F_S and F_T in Eq. (4), characterized by a different G-parity to the standard vector and axial currents of the Standard Model. The search for such currents has long been pursued in the β-decay experiments and in muon-capture experiments, but the measurement of polarization observables in the quasielastic scattering both of nucleons and of hyperons has been shown to be sensitive both to G invariance and to T-invariance [115]. Lattice QCD can contribute to these tests through calculations of induced scalar and tensor currents, including calculations of transition form factors to the rest of the SU(3) baryon octet (Λ and Σ as well as p and n), such as those in Refs. [116,117].

2.2 Moments of parton density functions

Lattice QCD can be used to calculate matrix elements of other operators besides the electroweak currents. An important class of operators are those that appear in the operator-product expansion of two currents. Their matrix elements are related to the moments of structure functions in deep-inelastic scattering. For a full discussion, see the USQCD companion white paper "Hadrons and Nuclei" [4]. Here, applications to neutrino physics are discussed.

In 2001, the NuTeV collaboration determined the on-shell weak mixing angle, $\sin^2\theta_W \equiv 1 - m_W^2/m_Z^2$, to be $0.2277 \pm 0.0013_{\rm stat} \pm 0.0009_{\rm syst}$ [118] in deep-inelastic neutrino scattering off iron. This result is 2.7σ discrepant from the current world average of other experiments, 0.22343 ± 0.00007 [64]. This discrepancy, which is known as the "NuTeV anomaly", has no universally accepted explanation, although many possibilities have been raised [119,120,121,122,123,124].

One suggestion that may account for part of the anomaly is the strange-antistrange parton asymmetry [125,126], $\langle x\rangle_{s_-} = \int dx\, x\,[s(x) - \bar{s}(x)]$, where $s(x)$ ($\bar{s}(x)$) is the (anti-)strange parton distribution function, as a function of parton momentum fraction x. A global analysis of several experimental data sets gives $\langle x\rangle_{s_-} \approx 0.0018$ [127], which is consistent with a 2006 NuTeV analysis of dimuon production [128]. The global analysis does not, however, find

a tight constraint: the authors of Ref. [127] present the range $-0.001 < \langle x \rangle_{s_-} < 0.005$ at 90% confidence level.

In view of the uncertainty in $\langle x \rangle_{s_-}$ from global fitting, a first-principles lattice-QCD calculation is clearly warranted. There is, however, no local operator which corresponds to $\langle x \rangle_{s_-}$. Instead, one can calculate the third moment from the local operator $\bar{s}\gamma_\mu D_\nu D_\lambda s$ which corresponds to $\langle x^2 \rangle_{s_-} = \int dx\, x^2 (s(x) - \bar{s}(x))$. Assuming $s(x) - \bar{s}(x)$ changes sign only once, $\langle x^2 \rangle_{s_-}$ should give the same sign as that of $\langle x \rangle_{s_-}$. This quantity can also be used to constrain the x-dependent distribution, but since it is expected to be small, calculations will require significant resources.

3 Challenging calculations

In this section, calculations that are computationally more difficult than the form factors in Sec. 2 are discussed. That said, the conceptual formalism underlying these calculations is well established, and pilot calculations provide some idea of how more complete calculations can be carried out. More complicated final states in the resonance regions (Sec. 3.1), the shallow inelastic region (Sec. 3.2), and the deep inelastic region (Sec. 3.3) are discussed, as are calculations of the axial charge, and related quantities, of small nuclei (Sec. 3.4).

3.1 Transition form factors: resonances and multibody final states

Neutrino scattering above the pion-production threshold constitutes the resonance region, where the scattered nucleon is excited into resonances, beginning with the $\Delta(1232)$. To describe the data in this regime thus requires a quantitative knowledge of the $N \to \Delta$ and $N \to N^*$ transitions, mediated through an external current. Because these hadrons are unstable, they can also be viewed as a nucleon with one or more pions, which are the only hadrons composed of the light u/d quarks stable under the strong interaction.

Lattice QCD has a long history of calculations of the transition form factors to the Δ, treating it as stable. Both the vector current [130,131], and the axial current [132] have been studied with unphysically large quark masses, such that M_Δ at these quark masses lies below the $N\pi$ threshold. These calculations are useful benchmarks for comparisons with non-lattice approaches that neglect the two-body nature of the resonance. Although not as rigorous as the methods discussed below, this "quick and dirty" approach may be timely, for example, providing qualitative input to understand better the MiniBooNE low-energy backgrounds from $\Delta \to N\gamma$ [133].

Because of the finite volume and Euclidean signature, calculations with two-body states in lattice QCD are conceptually and computationally more difficult [134,135,136] than the calculations discussed in Sec. 2. For example, the Lüscher method [134,135] relating energy shifts at finite volume to infinite-volume momentum-dependent phase shifts has been used to study the ρ meson [137,138,139,140,141], as well as $I = 2$ $\pi\pi$ phase shifts [142,143,144,145,146] from first principles. The theoretical framework for understanding the transition to multihadron states from Euclidean-space lattice QCD calculations have been further developed over the past several years. Notably, the formalism has been extended both to inelastic scattering [147,148,149,150,151] with several two-body channels, and to three-body scattering [152,153,154,155,156,157], and there have now been several computational applications of these advances [158,159,160,161].

A quantitative understanding of resonance production entails extending the formalism to encompassing transitions mediated through external currents, corresponding here to both vector and axial currents. The needed formalism to two-body final states, and for arbitrary spin, has now been developed [129]. The applications have largely focused on the meson sector. To cite an example bearing some similarity to $W^*n \to \Delta$ in neutrino scattering, the $\gamma^*\pi \to \rho$ transition has been computed in lattice QCD [162,163], providing the first rigorous calculation of the transition form factor to an unstable hadron, illustrated in Fig. 7. In addition, methods to extract resonance-to-resonance transitions, for example, $\gamma^*\rho \to \rho$, via lattice calculations of two-to-two transition amplitudes, in this case $\gamma^*\pi\pi \to \pi\pi$, have been developed [164,165]. This opens the possibility for calculations of two-body currents, that is, matrix elements of the form $\langle NN|J^\mu|NN\rangle$ needed for two-nucleon knockout.

Thus, the theoretical underpinnings for understanding resonance production in $\nu N \to \Delta$, N^*, and $N\pi$, are therefore largely in place. Calculations of multihadron states containing baryons are complicated by the extra complexity of the systems relating to the increased number of quarks, by poorer signal-to-noise ratios, and by the larger number of open channels. Even so, the first *ab initio* determination of $\Delta(1232)$ resonance parameters appeared in 2017 [166], albeit for a simulation with quark masses corresponding to a pion mass of 280 MeV, yield-

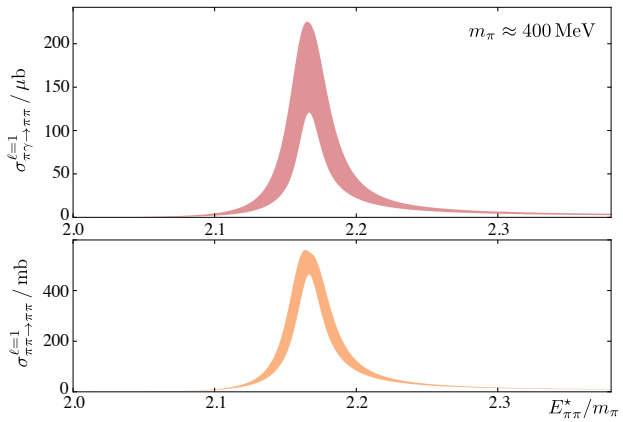

Fig. 7. The upper and lower panels show the $\gamma^*\pi^+ \to \pi^+\pi^0$ and $l = 1$ elastic $\pi\pi$ scattering cross sections, respectively, as a function of $\pi\pi$ energy, with the ρ resonance clearly visible [129].

ing a Δ-N-π coupling in agreement with phenomenological determinations. As the invariant mass of the system increases within the resonance regime and the pion mass is decreased to its physical value, however, inelastic processes and three- and higher-body final states become relevant. Further theoretical work is needed to encompass transitions to three or more particles, and further development of efficient algorithms is needed to evaluate the larger number of Wick contractions that increasingly dominate the computational cost of the calculation. The interplay between theoretical methods and practical algorithms is, of course, ideally researched on high-capacity computing facilities.

3.2 Hadron tensor for shallow and deep inelastic scattering

At higher energies, more and more pions are produced and a full theoretical description of any given final state becomes impractical. One can, however, study the sum over all final states via the optical theorem and consider forward matrix elements of the product of two currents. Whereas nuclear many-body theory decomposes the low-multiplicity cases into products of nuclear wavefunctions and nucleon (and $N\pi$, ...) form factors, here one can decompose the nuclear hadron tensor, $\langle A|J_\mu^\dagger J_\nu|A\rangle$, into a spectral function [167,168,169,170,171,172,173,174] and the nucleon hadron tensor, $\langle N|J_\mu^\dagger J_\nu|N\rangle$.[4] A recent development in lattice QCD is to calculate this quantity from a four-point correlation function. This approach is especially appealing in the region, sometimes called shallow inelastic, between the resonances and deep-inelastic scattering, where no other theoretical tool holds much promise [21].

The Euclidean hadronic tensor [179,180,181,182,183,184,185,186] can be decomposed in terms of structure functions that are related to their Minkowski counterparts through a Laplace transform. Thus, to obtain the desired structure functions, an inverse Laplace transform is needed, an ill-posed problem that arises in many fields. Three approaches to this problem are the maximum entropy method (MEM) [181], the MEM with a prior to stabilize the fit for Bayesian reconstruction (MEM-BR) [184], and the Backus-Gilbert method [186]. These three numerical approaches have been studied recently [187]. The Backus-Gilbert method yields a single broad peak in the energy spectrum from lattice data with 20 points in Euclidean time. With both the MEM and MEM-BR, the elastic peak and the resonance peak are resolved, with the MEM-BR producing sharper peaks and a more stable reconstruction. Given the test lattice spacing of 0.12 fm, there is no excitation spectrum above 2 GeV and, thus, no strength in the spectral weight above the resonance region. For a finer lattice with spacing 0.04 fm, the spectral weight up to 5 GeV is accessible. Even though it may still not be sufficient to resolve the individual resonances, the fact it can cover both the resonance and the shallow inelastic scattering regions makes the lattice hadronic tensor calculation a promising theoretical tool to address the total cross section of the neutrino-nucleus scattering over a wide range of energy transfers up to 5 GeV.

The hadron tensor can also be computed for deep-inelastic scattering. In this case, the calculation needs to be able to access the kinematic region where $Q^2 > 4$ GeV^2 and energy transfer $\nu > 5$ GeV where the higher-twist contributions are suppressed. The Euclidean correlation function can also be analyzed with the OPE, along the lines of the suggestion for calculating the shape function of the inclusive B-meson semileptonic decay rate [182]. In addition, using a fictitious heavy-quark propagator between the currents to calculate moments has been proposed [183]. A related approach is also discussed in Ref. [185]. Unlike the approaches discussed in the next subsection, the hadron-tensor approach to deep-inelastic scattering does not need to match to the infinite-momentum frame.

3.3 Parton densities for neutrino deep-inelastic scattering

The parton distribution functions (PDFs) will be important inputs in the upcoming precision neutrino-physics experiments, particularly at large Bjorken x and at the highest energies of the DUNE beam, $\sim$ 4–5 GeV. For these kinematics, current global-fit PDFs either suffer greatly from the theoretical uncertainty in their nuclear treatment or rely mainly on extrapolation from intermediate x.

Direct calculation of the Bjorken x dependence of hadron structure in lattice QCD has only recently become possible thanks to the development of the large-momentum effective theory (LaMET) [188], which introduces a large momentum P to connect Euclidean lattice QCD to the desired Minkowski distributions.[5] This framework has allowed the first direct lattice-QCD computations of the x dependence of parton distributions [195]. Further developments spurred on by these developments include that of pseudo-PDFs [196,197], and that of matrix elements of gauge-invariant current-current correlators [198,199]. In these new approaches, valence- and sea-quark structure can be disentangled, which leads to the possibility of using lattice-QCD calculations to directly compare with experiments on large-x structure in SoLID at Jefferson Lab, with sea structure in Drell-Yan experiments at Fermilab or with data from a future electron-ion collider. In addition to the hadron-tensor method described in the previous subsection, these new approaches and numerical investigations thereof are described in detail in the companion whitepaper "Hadrons and Nuclei" [4].

The lattice-QCD effort so far has focused on isovector combinations of PDFs, that is, the difference between the up and down distributions. A recent joint lattice-QCD and global-fitting community report [50], an effort led by USQCD members, demonstrated that a calculation of the

[4] The derivation of spectral functions of nuclear matter and finite nuclei is discussed in Refs. [175,176,177,178].

[5] See Refs. [189,190,191] for critical discussions of this approach and also Refs. [192,193,194] for the subsequent rebuttal of this criticism.

isovector proton PDF at the 12% level for $x \in [0.7, 0.9]$ can impact our knowledge of the PDF at x near 1 by more than 20%. This kinematic region is relevant for neutrino experiments, and such precision should be feasible in the near term. In addition, as crosscheck of nuclear theory in this region, exploratory calculations of nuclear PDFs will become available; see Sec. 3.4. Such precision is already relevant to neutrino-nucleon scattering at 4–5 GeV. Further, it allows a crosscheck of the nuclear-theory treatment and of the systematic uncertainties of nuclear PDFs.

Neutrino DIS can be important for determining the strange quark and antiquark parton distributions. Currently, no calculation of the Bjorken-x dependence of the strange PDF has been done with lattice QCD, due to numerical limitations, but there are USQCD proposals to investigate $s(x) - \bar{s}(x)$. On the other hand, the nucleon sea flavor asymmetry $\bar{u}(x) - \bar{d}(x)$ has been studied [200]. Unfortunately, the uncertainties in the quasi-PDF approach are currently much larger than those from experimental/phenomenological extraction.

Going to larger nucleon boost momenta P with high statistics is key to reducing several systematic uncertainties in these quasi- and pseudo-PDF approaches [4], especially for the antiquark distribution and small Bjorken x. However, this poses several computational challenges. First, large momentum translates into large $(aP)^n$, and therefore, ensembles with increasingly smaller lattice spacings a are needed. Given the need to keep the spatial size of the box sufficiently large to avoid significant finite-volume effects, which may be enhanced for some nonlocal matrix elements [201], this increases the computational cost. Second, as the momentum becomes larger, the signal-to-noise ratio degrades, even when using methods such as "momentum smearing" [202], designed to enhance the contribution of the lowest-lying state in correlation functions at nonzero three-momentum, thereby increasing the number of measurements that need to be made. Third, the excited-state contributions themselves become more significant at higher momenta both through the greater number of contributing states arising from the reduced symmetries at nonzero momentum, and through the relative compression of the energy spectrum. This requires either calculations at many source-sink separations, or the use of the variational method with an expanded basis of operators. Finally, one must address the inverse problem involving a Laplace, Fourier, or Mellin transform of a certain class of position-space matrix elements. For example, in the case of quasi- and pseudo-PDFs, spurious oscillations can be introduced when Fourier transforming the "Ioffe" time variable. Several methods of advanced reconstructions have been analyzed to overcome this challenge [203] and clearly further research is needed here. Thus, calculations of the precision that the neutrino program demands requires a significant commitment of computational resources.

3.4 Axial currents in light nuclei

An important challenge for lattice QCD is to extend the calculations of the axial properties of the nucleon to the more complex systems of nuclei. Just as for the nucleon, knowing nuclear matrix elements of axial currents and of quantities relevant in deep-inelastic scattering on nuclei are high priorities in the lattice-QCD community. Over the last decade, first studies of a range of nuclear properties have been performed, and calculations of the requisite axial structure of light nuclei are eminently feasible in a five-year timeframe.

Nuclear effects in neutrino-nucleus scattering are important, extremely nontrivial, and not simply related to those in electron-nucleus scattering. For example, Gamow-Teller transitions in nuclei [204,205,206], which flip spin and isospin of the nucleus, are poorly described in most simple nuclear models, with deviations of as much as 25% from naive expectations based on simply scaling from the single-particle $n \to pe\bar{\nu}$ transition. Once sophisticated nuclear wave functions and many-body axial currents [207, 208] are used, however, agreement with the data is reached [209]. At higher energies, state-of-the-art Green-function Monte-Carlo (an exact many-body method) calculations [210, 211] show that neutrino response functions describing scattering on nuclei such as ^{12}C have effects from two-body currents at the 20% level, particularly in the transverse response.

In the last few years, USQCD collaboration members have performed lattice-QCD calculations of $A = 2, 3$ axial transitions in the forward limit using unphysically heavy quark masses corresponding to $M_\pi \sim 800$ MeV [212,213, 214]. This work, in which the Gamow-Teller contribution to tritium β-decay and the rate of the $pp \to de\bar{\nu}$ fusion process were extracted, demonstrates that the calculations relevant to constrain neutrino interactions with light nuclei can be performed. While nuclear effects in the axial matrix elements of two- and three-body systems are found to be at the few percent level, the lattice-QCD calculations were able to resolve the relevant effects by isolating the intrinsically two-body contributions. Pursuing these calculations at the physical quark masses and controlling all sources of systematic uncertainties in them will require exascale computing resources. Beyond these forward limit calculations, extensions of this approach to enable calculations of the form factors of light nuclei from nonforward transition matrix elements are underway. Calculations involving multiparticle final states are also necessary but challenging: a theoretical understanding of the simplest inelastic channels is presented in Ref. [164]. For high-energy neutrino-nucleus scattering in the deep-inelastic regime, lattice-QCD calculations of the moments of the relevant parton distributions in nuclei will be useful in constraining nuclear effects in a very different kinematic regime.

While these calculations do not directly address the particular nuclear targets for DUNE and other neutrino-scattering experiments, they are useful in constraining the low-energy constants and meson-exchange currents that enter nuclear-chiral-EFT axial currents [207,208]. Such matchings are already underway for spectroscopy [215, 216,217] and electromagnetic interactions [218] at unphysical values of the quark masses, and the machinery necessary to undertake this at the physical quark masses is be-

ing developed. As well as studies of currents, lattice-QCD calculations of nuclei and other systems such as three and four neutron systems will provide input into the three-body forces in nuclear EFTs, particularly those aspects of these forces that are challenging to access experimentally.

4 Extremely challenging calculations

Looking further into the future, we can foresee the need for calculations that go far enough beyond the current state of the art that it is hard to know when or whether they will be possible.

4.1 Electromagnetic and isospin-breaking effects

Going beyond the leading order, calculations of nucleon matrix elements must incorporated the neglected contributions from both QED and from strong isospin breaking (SIB). There are two possible approaches for completing these tasks, which can be generally classified as being perturbative and nonperturbative. Perturbative calculations make use of existing isospin-symmetric and QCD-only lattice ensembles to compute the desired matrix elements. The QED effects are computed with explicit vector current insertions and some scheme for the virtual photon lines. Similarly, the SIB effects are included via scalar current insertions that allow for expansion in quark mass about the isospin-symmetric point. For nucleon matrix elements, perturbative calculations require five-point correlation functions as well as disconnected diagrams and and pose a significant challenge to pursue.

Nonperturbative calculations make use of gauge ensembles that include explicit sea effects for QED and SIB. These are $\mathrm{SU}(3) \times \mathrm{U}(1)$ gauge field ensembles with the up and down quark masses tuned to their physical values. Rather than being restricted to a perturbative expansion of photon fields, these calculations include combined gluon, photon, and quark loops to all orders. While these calculations are likely to be cheaper than the perturbative calculations mentioned above, they also have technical difficulties that must be overcome. The most challenging of these difficulties is likely to come from finite size effects. Since photons mediate a long range force, calculations including QED will be sensitive to the size of the lattice. Many computations on lattice ensembles with different volumes will be necessary to quantify and remove this systematic effect.

4.2 Axial currents in heavier nuclei

A holy grail for neutrino-nucleus scattering is controlled QCD calculations of the axial form factors, resonance transition form factors, and nuclear PDFs for ^{40}Ar, the target nucleus in DUNE and several other experiments. As yet, exponentially hard challenges must be overcome in order for meaningful lattice-QCD calculations of such heavy nuclei. Both the factorial growth complexity of many-body contractions and the exponentially degradation of the signal-to-noise ratio are currently impede to progress on this front. Since lattice-QCD studies of nuclei are relatively new, it is not unlikely that new algorithms will definitively alter this picture (algorithms involving machine learning and quantum computation [219] may dramatically improve the situation),[6] but at present it is realistic to assume that direct lattice-QCD calculations of argon will not occur in a timeframe relevant for the coming long-baseline experiments.

Perhaps more realistically, significant tests of nuclear EFT frameworks beyond the few-body sector would be enabled by lattice-QCD calculations of the spectrum and axial structure of an intermediate nucleus such as ^{12}C. Aspects of coherent scattering off nuclei will also be addressed by such calculations. While still challenging, a number of groups are investigating ways to perform the relevant contractions and studying improved ways to extract signals from noisy multi-baryon data through optimization methods [220] or improved estimators [221,56,222,223,224]. For carbon targets, experimental scattering data exists and comparison of lattice-QCD calculations with this will help understand the systematics of the A dependence of nuclear EFT approaches and assess the reliability of the extrapolations to argon.

For light nuclei, adapting the techniques discussed above to address the Bjorken-x dependence on nuclear PDFs will become possible as computing resources increase. While challenging, and still in the development stage even for the nucleon, these PDF methods will help constrain the flavor and spin dependence of nuclear PDFs that are important for high-energy νA scattering.

5 Computing needs

As we have seen in Secs. 3 and 4, many topics pertaining to lattice QCD for neutrino physics are still exploratory. In those cases, computing estimates are impossible because progress depends on innovation and flexible computing, rather than an industrial resource. It is feasible and reasonable, however, to estimate the computing needs of the calculations discussed in Sec. 2. We do so here, focusing on the example of nucleon form factors.

The methodology for the calculation of the axial and the electromagnetic form factors is well established, and data with control over statistical errors have been generated by several collaborations worldwide. Table 1 list several of these efforts. Unfortunately, only a few include several ensembles with strange sea quarks [87,81,84]. Even those calculations should be pushed to smaller lattice spacing and (in one case) smaller up-down quark mass. Furthermore, most calculations obtain mean-squared charge radii (r_A, r_E, and r_M) that are smaller than phenomenological extractions, by about 30%. To diagnose where the

[6] For discussion of these novel approaches, see the companion whitepaper "Status and Future Perspectives for Lattice Gauge Theory Calculations to the Exascale and Beyond" [5].

difference lies, it is crucial to improve control over systematic uncertainties in lattice-QCD calculations to obtain a definitive result from QCD.

Here we base the cost estimates for achieving a 10–15% result on two ongoing efforts within USQCD. A convenient starting point is the work of PNDME collaboration that has presented extensive results for the axial form factors [81] using the Wilson-clover formulation for the valence quarks on ensembles with 2+1+1 sea quarks with the staggered formulation. One way to avoid this "mixed action" approach is to use staggered valence quarks [100]. Based on current running on institutional clusters at BNL and Fermilab, we estimate 9M GPU-hours[7] to carry out a calculation on eleven ensembles, five at physical sea-quark mass, and six with $m_l = \frac{1}{2}(m_u+m_d) = 0.2m_s$, with lattice spacing as small as 0.03 fm.

Similarly, a significant subset of USQCD plans on generating a suite of ensembles with Wilson-clover sea quarks. To generate eight such ensembles, with light sea-quark masses corresponding to pion masses of 170 MeV and 270 MeV (four ensembles each), with lattice spacing as small as 0.05 fm. The estimate to finish generating these ensembles is 8M GPU-hours (assuming the GPUs on Summit at ORNL). This chunk of computing will be shared with many other projects, particularly those described in the companion white paper "Hadrons and Nuclei" [4]. The computation of the needed nucleon correlation functions is estimated to require 15M GPU-hours.

These estimates set the scale for a modern calculation of the simplest quantity needed for neutrino physics. At the same time, comparably demanding work with small nuclei, but not yet physical pion mass, will be needed. Such work is necessary to understand the technical issues facing more realistic calculations and to find better methods and algorithms. Even assuming gains from innovation, it is hard to imagine that nuclear form factors will end up below 10M GPU-hours. The same line of reasoning can be applied to other calculations discussed in Sec. 3.

We would like to thank Raúl Briceño, Maxwell Hansen, Richard Hill, Ciaran Hughes, Peter Kammel, William Marciano, Saori Pastore, Noemi Rocco, Michael Wagman, and Savvas Zafeiropoulos for useful input. This material is co-authored by employees of Jefferson Science Assocates supported by the U.S. Department of Energy, Office of Science, Office of Nuclear Physics under contract No. DE-AC05-06OR23177, by employees of Fermi Research Alliance, LLC, under Contract No. DE-AC02-07CH11359 with the U.S. Department of Energy, Office of Science, Office of High Energy Physics, and by employees of Brookhaven Science Associates, LLC, under Contract No. DE-SC0012704 with the U.S. Departmernt of Energy. RG is supported in part by the U.S. Department of Energy, Office of Science, Office of High Energy Physics under Contract No. DE-AC52-06NA25396, and by the LANL LDRD program. SS is supported by the National Science Foundation under CAREER Award PHY-1847893 and by the RHIC Physics Fellow Program of the RIKEN BNL Research Center. HL is supported by the US National Science Foundation under grant PHY-1653405 "CAREER: Constraining Parton Distribution Functions for New-Physics Searches"

[7] For QCD codes, these 9M GPU hours correspond to 300M conventional (e.g., Intel Skylake) CPU core-hours.

References

1. A. Bazavov, F. Karsch, S. Mukherjee, P. Petreczky (USQCD) (2019), 1904.09951
2. R. Brower, A. Hasenfratz, E.T. Neil, S. Catterall, G. Fleming, J. Giedt, E. Rinaldi, D. Schaich, E. Weinberg, O. Witzel (USQCD) (2019), 1904.09964
3. V. Cirigliano, Z. Davoudi, T. Bhattacharya, T. Izubuchi, P.E. Shanahan, S. Syritsyn, M.L. Wagman (USQCD) (2019), 1904.09704
4. W. Detmold, R.G. Edwards, J.J. Dudek, M. Engelhardt, H.W. Lin, S. Meinel, K. Orginos, P. Shanahan (USQCD) (2019), 1904.09512
5. B. Joó, C. Jung, N.H. Christ, W. Detmold, R. Edwards, M. Savage, P. Shanahan (USQCD), Phys. Rev. (2019), 1904.09725
6. C. Lehner, S. Meinel, T. Blum, N.H. Christ, A.X. El-Khadra, M.T. Hansen, A.S. Kronfeld, J. Laiho, E.T. Neil, S.R. Sharpe et al. (USQCD) (2019), 1904.09479
7. Y. Fukuda et al. (Super-Kamiokande), Phys. Rev. Lett. **81**, 1562 (1998), hep-ex/9807003
8. Q.R. Ahmad et al. (SNO), Phys. Rev. Lett. **87**, 071301 (2001), nucl-ex/0106015
9. R. Acciarri et al. (DUNE) (2015), 1512.06148
10. K. Abe et al. (Hyper-Kamiokande) (2018), 1805.04163
11. E. Majorana, Nuovo Cim. **14**, 171 (1937)
12. P. Minkowski, Phys. Lett. **67B**, 421 (1977)
13. T. Yanagida, Prog. Theor. Phys. **64**, 1103 (1980)
14. M. Gell-Mann, P. Ramond, R. Slansky, *Complex Spinors and Unified Theories* (North-Holland, Amsterdam, 1979), pp. 315–321, 1306.4669
15. B. Pontecorvo, Sov. Phys. JETP **6**, 429 (1957), [Zh. Eksp. Teor. Fiz. **33**, 549 (1957)]
16. B. Pontecorvo, Sov. Phys. JETP **26**, 984 (1968), [Zh. Eksp. Teor. Fiz. **53**, 1717 (1967)]
17. Z. Maki, M. Nakagawa, S. Sakata, Prog. Theor. Phys. **28**, 870 (1962)
18. N. Cabibbo, Phys. Rev. Lett. **10**, 531 (1963)
19. M. Kobayashi, T. Maskawa, Prog. Theor. Phys. **49**, 652 (1973)
20. L. Fields, private communication (2018)
21. L. Alvarez-Ruso et al. (NuSTEC), Prog. Part. Nucl. Phys. **100**, 1 (2018), 1706.03621
22. O. Benhar, A. Lovato, Int. J. Mod. Phys. **E24**, 1530006 (2015), 1506.05225
23. J. Carlson, S. Gandolfi, F. Pederiva, S.C. Pieper, R. Schiavilla, K.E. Schmidt, R.B. Wiringa, Rev. Mod. Phys. **87**, 1067 (2015), and references within, 1412.3081
24. E. Epelbaum, H.W. Hammer, U.G. Meissner, Rev. Mod. Phys. **81**, 1773 (2009), 0811.1338
25. R. Machleidt, D.R. Entem, Phys. Rept. **503**, 1 (2011), 1105.2919
26. S. Weinberg, Phys. Lett. **B251**, 288 (1990)
27. U. van Kolck, Phys. Rev. **C49**, 2932 (1994)
28. D.B. Kaplan, M.J. Savage, M.B. Wise, Phys. Lett. **B424**, 390 (1998), nucl-th/9801034
29. U.G. Meißner, Phys. Scripta **91**, 033005 (2016), 1510.03230

Table 1. Sample of calculations of nucleon form factors going on worldwide. In the first column, "2", "2+1", and "2+1+1" all denote two equal-mass quarks for up and down; the latter two include strange and charm, respectively. The last column indicates work in which USQCD members participate.

Sea quarks	Valence quarks	$N_{\rm ens}$	a (fm)	M_π (MeV)	Collaboration	Ref.	USQCD
2 Wilson-clover	same as sea	11	0.06–0.08	150–490	RQCD	[76]	
2 TM clover	same as sea	1	0.09	130	ETM	[79]	
2 Wilson-clover	same as sea	11	0.05–0.08	190–470	Mainz (CLS)	[80]	
2+1 overlap	same as sea	4	0.11	290–540	JLQCD	[83]	
2+1 domain wall [60]	overlap	3	0.08–0.15	170–340	χQCD	[86]	✓
2+1 Wilson-clover	same as sea	1	0.085	146, 135	PACS	[89]	
2+1 Wilson-clover	same as sea	11	0.05–0.09	200–350	Mainz (CLS)	[87]	
2+1+1 HISQ [52]	Wilson-clover	8	0.06–0.12	135–210	PNDME	[81]	✓
2+1+1 HISQ [52]	domain wall	16	0.09–0.15	130–400	CalLat	[84]	✓
2+1+1 TM clover	same as sea	3	0.09–0.15	140	ETM	[90]	✓
2+1+1 HISQ	same as sea	3	0.09–0.15	135	Fermilab/MILC	[100]	✓

30. C. Juszczak, J.A. Nowak, J.T. Sobczyk, Nucl. Phys. Proc. Suppl. **159**, 211 (2006), hep-ph/0512365
31. J. Żmuda, K.M. Graczyk, C. Juszczak, J.T. Sobczyk, Acta Phys. Polon. **B46**, 2329 (2015), 1510.03268
32. Y. Hayato, Acta Phys. Polon. **B40**, 2477 (2009)
33. C. Andreopoulos et al., Nucl. Instrum. Meth. **A614**, 87 (2010), 0905.2517
34. M. Alam et al., *GENIE production release 2.10.0* (2015), 1512.06882
35. K. Gallmeister, U. Mosel, J. Weil, Phys. Rev. **C94**, 035502 (2016), 1605.09391
36. D. Casper, Nucl. Phys. Proc. Suppl. **112**, 161 (2002), hep-ph/0208030
37. J. Morfín, *Past and future of $\nu/\bar{\nu}$ deuterium/hydrogen experiments*, talk at INT Seattle (2018)
38. D. Androić et al. (Qweak), Nature **557**, 207 (2018)
39. D.Z. Freedman, Phys. Rev. **D9**, 1389 (1974)
40. S.J. Brice et al., Phys. Rev. **D89**, 072004 (2014), 1311.5958
41. D. Akimov et al. (COHERENT), Science **357**, 1123 (2017), 1708.01294
42. J.A. Formaggio, G.P. Zeller, Rev. Mod. Phys. **84**, 1307 (2012), 1305.7513
43. J. Carlson, R. Schiavilla, Rev. Mod. Phys. **70**, 743 (1998)
44. S. Bacca, S. Pastore, J. Phys. **G41**, 123002 (2014), 1407.3490
45. R. Gran, J. Nieves, F. Sanchez, M.J. Vicente Vacas, Phys. Rev. **D88**, 113007 (2013), 1307.8105
46. O. Benhar, A. Lovato, N. Rocco, Phys. Rev. **C92**, 024602 (2015), 1502.00887
47. G.D. Megias, J.E. Amaro, M.B. Barbaro, J.A. Caballero, T.W. Donnelly, I. Ruiz Simo, Phys. Rev. **D94**, 093004 (2016), 1607.08565
48. T. Van Cuyck, N. Jachowicz, R. González-Jiménez, J. Ryckebusch, N. Van Dessel, Phys. Rev. **C95**, 054611 (2017), 1702.06402
49. A.V. Butkevich, S.V. Luchuk, Phys. Rev. **C97**, 045502 (2018), 1708.04052
50. H.W. Lin et al., Prog. Part. Nucl. Phys. **100**, 107 (2018), 1711.07916
51. S. Dürr et al. (Budapest-Marseille-Wuppertal), JHEP **08**, 148 (2011), 1011.2711
52. A. Bazavov et al. (MILC), Phys. Rev. **D87**, 054505 (2013), 1212.4768
53. A. Bazavov et al. (Fermilab Lattice, MILC), Phys. Rev. **D98**, 074512 (2018), 1712.09262
54. G. Parisi, Phys. Rept. **103**, 203 (1984)
55. G.P. Lepage, *The Analysis of Algorithms for Lattice Field Theory*, in *From Actions to Answers*, edited by T. DeGrand, W.D. Toussaint (World Scientific, Singapore, 1989), pp. 97–120
56. M.L. Wagman, Ph.D. thesis, University of Washington (2017), 1711.00062
57. B.J. Owen, J. Dragos, W. Kamleh, D.B. Leinweber, M.S. Mahbub, B.J. Menadue, J.M. Zanotti, Phys. Lett. **B723**, 217 (2013), 1212.4668
58. B. Yoon et al., Phys. Rev. **D93**, 114506 (2016), 1602.07737
59. C. Egerer, D. Richards, F. Winter, Phys. Rev. **D99**, 034506 (2019), 1810.09991
60. T. Blum et al. (RBC, UKQCD), Phys. Rev. **D93**, 074505 (2016), 1411.7017
61. B. Bhattacharya, R.J. Hill, G. Paz, Phys. Rev. **D84**, 073006 (2011), 1108.0423
62. S. Weinberg, Phys. Rev. **112**, 1375 (1958)
63. C.H. Llewellyn Smith, Phys. Rept. **3**, 261 (1972)
64. M. Tanabashi et al. (Particle Data Group), Phys. Rev. **D98**, 030001 (2018)
65. A. Bodek, S. Avvakumov, R. Bradford, H.S. Budd, Eur. Phys. J. **C53**, 349 (2008), 0708.1946
66. A. Liesenfeld et al. (A1), Phys. Lett. **B468**, 20 (1999), nucl-ex/9911003
67. V. Bernard, N. Kaiser, U.G. Meissner, Phys. Rev. Lett. **69**, 1877 (1992)
68. R. Gran et al. (K2K), Phys. Rev. **D74**, 052002 (2006), hep-ex/0603034
69. M. Dorman (MINOS), AIP Conf. Proc. **1189**, 133 (2009)
70. A.A. Aguilar-Arevalo et al. (MiniBooNE), Phys. Rev. **D81**, 092005 (2010), 1002.2680
71. V. Lyubushkin et al. (NOMAD), Eur. Phys. J. **C63**, 355 (2009), 0812.4543
72. L. Fields et al. (MINERvA), Phys. Rev. Lett. **111**, 022501 (2013), 1305.2234
73. G.A. Fiorentini et al. (MINERvA), Phys. Rev. Lett. **111**, 022502 (2013), 1305.2243
74. A.S. Meyer, M. Betancourt, R. Gran, R.J. Hill, Phys. Rev. **D93**, 113015 (2016), 1603.03048
75. R.J. Hill, P. Kammel, W.J. Marciano, A. Sirlin, Rept. Prog. Phys. **81**, 096301 (2018), 1708.08462

76. G.S. Bali, S. Collins, B. Gläßle, M. Göckeler, J. Najjar, R.H. Rödl, A. Schäfer, R.W. Schiel, W. Söldner, A. Sternbeck, Phys. Rev. **D91**, 054501 (2015), 1412.7336
77. T. Bhattacharya, V. Cirigliano, S. Cohen, R. Gupta, H.W. Lin, B. Yoon, Phys. Rev. **D94**, 054508 (2016), 1606.07049
78. J. Green, N. Hasan, S. Meinel, M. Engelhardt, S. Krieg, J. Laeuchli, J. Negele, K. Orginos, A. Pochinsky, S. Syritsyn, Phys. Rev. **D95**, 114502 (2017), 1703.06703
79. C. Alexandrou, M. Constantinou, K. Hadjiyiannakou, K. Jansen, C. Kallidonis, G. Koutsou, A. Vaquero Aviles-Casco, Phys. Rev. **D96**, 054507 (2017), 1705.03399
80. S. Capitani, M. Della Morte, D. Djukanovic, G.M. von Hippel, J. Hua, B. Jäger, P.M. Junnarkar, H.B. Meyer, T.D. Rae, H. Wittig, Int. J. Mod. Phys. **A34**, 1950009 (2019), 1705.06186
81. R. Gupta, Y.C. Jang, H.W. Lin, B. Yoon, T. Bhattacharya (PNDME), Phys. Rev. **D96**, 114503 (2017), 1705.06834
82. Y.C. Jang, T. Bhattacharya, R. Gupta, H.W. Lin, B. Yoon, EPJ Web Conf. **175**, 06033 (2018), 1801.01635
83. N. Yamanaka, S. Hashimoto, T. Kaneko, H. Ohki (JLQCD), Phys. Rev. **D98**, 054516 (2018), 1805.10507
84. C.C. Chang et al. (CalLat), Nature **558**, 91 (2018), 1805.12130
85. K.I. Ishikawa, Y. Kuramashi, S. Sasaki, N. Tsukamoto, A. Ukawa, T. Yamazaki (PACS), Phys. Rev. **D98**, 074510 (2018), 1807.03974
86. J. Liang, Y.B. Yang, T. Draper, M. Gong, K.F. Liu (χQCD), Phys. Rev. **D98**, 074505 (2018), 1806.08366
87. K. Ottnad, T. Harris, H. Meyer, G. von Hippel, J. Wilhelm, H. Wittig, PoS **LATTICE2018**, 129 (2018), 1809.10638
88. G.S. Bali, S. Collins, M. Gruber, A. Schäfer, P. Wein, T. Wurm (RQCD), Phys. Lett. **B789**, 666 (2019), 1810.05569
89. E. Shintani, K.I. Ishikawa, Y. Kuramashi, S. Sasaki, T. Yamazaki (PACS), Phys. Rev. **D99**, 014510 (2019), 1811.07292
90. M. Constantinou, C. Alexandrou, S. Bacchio, K. Hadjiyiannakou, K. Jansen, G. Koutsou, A. Vaquero Aviles-Casco, PoS **LATTICE2018**, 142 (2018)
91. Y.C. Jang, T. Bhattacharya, R. Gupta, H.W. Lin, B. Yoon (PNDME), PoS **LATTICE2018**, 123 (2018), 1901.00060
92. V. Bernard, L. Elouadrhiri, U.G. Meissner, J. Phys. **G28**, R1 (2002), hep-ph/0107088
93. R. Gupta, Y.C. Jang, B. Yoon, H.W. Lin, V. Cirigliano, T. Bhattacharya (PNDME), Phys. Rev. **D98**, 034503 (2018), 1806.09006
94. S. Aoki et al. (Flavor Lattice Averaging Group), Eur. Phys. J. **C77**, 112 (2017), 1607.00299
95. S. Aoki et al. (Flavour Lattice Averaging Group) (2019), 1902.08191
96. updates can be found on the FLAG website
97. T. Bhattacharya, V. Cirigliano, S. Cohen, R. Gupta, A. Joseph, H.W. Lin, B. Yoon (PNDME), Phys. Rev. **D92**, 094511 (2015), 1506.06411
98. S. Arzumanov, L. Bondarenko, S. Chernyavsky, P. Geltenbort, V. Morozov, V.V. Nesvizhevsky, Yu. Panin, A. Strepetov, Phys. Lett. **B745**, 79 (2015)
99. A.T. Yue, M.S. Dewey, D.M. Gilliam, G.L. Greene, A.B. Laptev, J.S. Nico, W.M. Snow, F.E. Wietfeldt, Phys. Rev. Lett. **111**, 222501 (2013), 1309.2623
100. A.S. Meyer, R.J. Hill, A.S. Kronfeld, R. Li, J.N. Simone, PoS **LATTICE2016**, 179 (2016), 1610.04593
101. N.N. Meiman, Sov. Phys. JETP **17**, 830 (1963), [Zh. Eksp. Teor. Fiz. **44**, 1228 (1963)]
102. R.J. Hill, G. Paz, Phys. Rev. **D82**, 113005 (2010), 1008.4619
103. R.J. Hill, eConf **C060409**, 027 (2006), hep-ph/0606023
104. C. Bernard et al. (Fermilab Lattice, MILC), Phys. Rev. **D79**, 014506 (2009), 0808.2519
105. J.A. Bailey et al. (Fermilab Lattice, MILC), Phys. Rev. **D79**, 054507 (2009), 0811.3640
106. A. de Gouvêa, K.J. Kelly, Nucl. Phys. **B908**, 318 (2016), 1511.05562
107. J. Heeck, M. Lindner, W. Rodejohann, S. Vogl, SciPost Phys. **6**, 038 (2019), 1812.04067
108. D.S. Armstrong, R.D. McKeown, Annu. Rev. Nucl. Part. Sci. **62**, 337 (2012), 1207.5238
109. Z. Ye, J. Arrington, R.J. Hill, G. Lee, Phys. Lett. **B777**, 8 (2018), 1707.09063
110. R.S. Sufian, Phys. Rev. **D96**, 093007 (2017), 1611.07031
111. G. Garvey, E. Kolbe, K. Langanke, S. Krewald, Phys. Rev. **C48**, 1919 (1993)
112. G.T. Garvey, W.C. Louis, D.H. White, Phys. Rev. **C48**, 761 (1993)
113. A.A. Aguilar-Arevalo et al. (MiniBooNE), Phys. Rev. **D82**, 092005 (2010), 1007.4730
114. A.A. Aguilar-Arevalo et al. (MiniBooNE), Phys. Rev. **D91**, 012004 (2015), 1309.7257
115. A. Fatima, M. Sajjad Athar, S.K. Singh, Phys. Rev. **D98**, 033005 (2018), 1806.08597
116. H.W. Lin, Nucl. Phys. Proc. Suppl. **187**, 200 (2009), 0812.0411
117. S. Sasaki, PoS **LATTICE2013**, 388 (2014)
118. G.P. Zeller et al. (NuTeV), Phys. Rev. Lett. **88**, 091802 (2002), **90**, 239902E (2003), hep-ex/0110059
119. J.T. Londergan, A.W. Thomas, Phys. Rev. **D67**, 111901 (2003), hep-ph/0303155
120. Y. Ding, R.G. Xu, B.Q. Ma, Phys. Lett. **B607**, 101 (2005), hep-ph/0408292
121. M. Gluck, P. Jimenez-Delgado, E. Reya, Phys. Rev. Lett. **95**, 022002 (2005), hep-ph/0503103
122. K.J. Eskola, H. Paukkunen, JHEP **06**, 008 (2006), hep-ph/0603155
123. I.C. Cloet, W. Bentz, A.W. Thomas, Phys. Rev. Lett. **102**, 252301 (2009), 0901.3559
124. W. Bentz, I.C. Cloet, J.T. Londergan, A.W. Thomas, Phys. Lett. **B693**, 462 (2010), 0908.3198
125. S. Davidson, S. Forte, P. Gambino, N. Rius, A. Strumia, JHEP **02**, 037 (2002), hep-ph/0112302
126. S. Kretzer, F. Olness, J. Pumplin, D. Stump, W.K. Tung, M.H. Reno, Phys. Rev. Lett. **93**, 041802 (2004), hep-ph/0312322
127. H.L. Lai, P.M. Nadolsky, J. Pumplin, D. Stump, W.K. Tung, C.P. Yuan, JHEP **04**, 089 (2007), hep-ph/0702268
128. D.A. Mason, Ph.D. thesis, University of Oregon (2006), http://lss.fnal.gov/archive/thesis/2000/fermilab-thesis-20
129. R.A. Briceño, M.T. Hansen, Phys. Rev. **D92**, 074509 (2015), 1502.04314
130. D.B. Leinweber, T. Draper, R.M. Woloshyn, Phys. Rev. **D48**, 2230 (1993), hep-lat/9212016
131. C. Alexandrou, G. Koutsou, H. Neff, J.W. Negele, W. Schroers, A. Tsapalis, Phys. Rev. **D77**, 085012 (2008), 0710.4621

132. C. Alexandrou, G. Koutsou, T. Leontiou, J.W. Negele, A. Tsapalis, Phys. Rev. **D76**, 094511 (2007), [**D80**, 099901 (2009)], 0706.3011
133. A.A. Aguilar-Arevalo et al. (MiniBooNE), Phys. Rev. Lett. **121**, 221801 (2018), 1805.12028
134. M. Lüscher, Commun. Math. Phys. **105**, 153 (1986)
135. M. Lüscher, Nucl. Phys. **B354**, 531 (1991)
136. L. Lellouch, M. Lüscher, Commun. Math. Phys. **219**, 31 (2001), hep-lat/0003023
137. S. Aoki et al. (CP-PACS), Phys. Rev. **D76**, 094506 (2007), 0708.3705
138. X. Feng, K. Jansen, D.B. Renner, Phys. Rev. **D83**, 094505 (2011), 1011.5288
139. J.J. Dudek, R.G. Edwards, C.E. Thomas (Hadron Spectrum), Phys. Rev. **D87**, 034505 (2013), [Erratum: Phys. Rev.D90,no.9,099902(2014)], 1212.0830
140. D.J. Wilson, R.A. Briceño, J.J. Dudek, R.G. Edwards, C.E. Thomas, Phys. Rev. **D92**, 094502 (2015), 1507.02599
141. C. Alexandrou, L. Leskovec, S. Meinel, J. Negele, S. Paul, M. Petschlies, A. Pochinsky, G. Rendon, S. Syritsyn, Phys. Rev. **D96**, 034525 (2017), 1704.05439
142. S.R. Beane, T.C. Luu, K. Orginos, A. Parreno, M.J. Savage, A. Torok, A. Walker-Loud, Phys. Rev. **D77**, 014505 (2008), 0706.3026
143. X. Feng, K. Jansen, D.B. Renner, Phys. Lett. **B684**, 268 (2010), 0909.3255
144. S.R. Beane, E. Chang, W. Detmold, H.W. Lin, T.C. Luu, K. Orginos, A. Parreno, M.J. Savage, A. Torok, A. Walker-Loud (NPLQCD), Phys. Rev. **D85**, 034505 (2012), 1107.5023
145. J.J. Dudek, R.G. Edwards, M.J. Peardon, D.G. Richards, C.E. Thomas, Phys. Rev. **D83**, 071504 (2011), 1011.6352
146. J.J. Dudek, R.G. Edwards, C.E. Thomas, Phys. Rev. **D86**, 034031 (2012), 1203.6041
147. W. Detmold, M.J. Savage, Nucl. Phys. **A743**, 170 (2004), hep-lat/0403005
148. S. He, X. Feng, C. Liu, JHEP **07**, 011 (2005), hep-lat/0504019
149. M.T. Hansen, S.R. Sharpe, Phys. Rev. **D86**, 016007 (2012), 1204.0826
150. R.A. Briceño, Z. Davoudi, Phys. Rev. **D88**, 094507 (2013), 1204.1110
151. P. Guo, J. Dudek, R. Edwards, A.P. Szczepaniak, Phys. Rev. **D88**, 014501 (2013), 1211.0929
152. S. Kreuzer, H.W. Hammer, Phys. Lett. **B694**, 424 (2011), 1008.4499
153. R.A. Briceño, Z. Davoudi, Phys. Rev. **D87**, 094507 (2013), 1212.3398
154. U.G. Meißner, G. Ríos, A. Rusetsky, Phys. Rev. Lett. **114**, 091602 (2015), [Erratum: Phys. Rev. Lett.117,no.6,069902(2016)], 1412.4969
155. R.A. Briceño, M.T. Hansen, S.R. Sharpe, Phys. Rev. **D95**, 074510 (2017), 1701.07465
156. R.A. Briceño, M.T. Hansen, S.R. Sharpe, Phys. Rev. **D99**, 014516 (2019), 1810.01429
157. M. Döring, H.W. Hammer, M. Mai, J.Y. Pang, A. Rusetsky, J. Wu, Phys. Rev. **D97**, 114508 (2018), 1802.03362
158. S.R. Beane, W. Detmold, T.C. Luu, K. Orginos, M.J. Savage, A. Torok, Phys. Rev. Lett. **100**, 082004 (2008), 0710.1827
159. J.J. Dudek, R.G. Edwards, D.J. Wilson (Hadron Spectrum), Phys. Rev. **D93**, 094506 (2016), 1602.05122
160. R.A. Briceño, J.J. Dudek, R.G. Edwards, D.J. Wilson (Hadron Spectrum), Phys. Rev. **D97**, 054513 (2018), 1708.06667
161. A. Woss, C.E. Thomas, J.J. Dudek, R.G. Edwards, D.J. Wilson (Hadron Spectrum), JHEP **07**, 043 (2018), 1802.05580
162. R.A. Briceño, J.J. Dudek, R.G. Edwards, C.J. Shultz, C.E. Thomas, D.J. Wilson, Phys. Rev. **D93**, 114508 (2016), 1604.03530
163. C. Alexandrou, L. Leskovec, S. Meinel, J. Negele, S. Paul, M. Petschlies, A. Pochinsky, G. Rendon, S. Syritsyn, Phys. Rev. **D98**, 074502 (2018), 1807.08357
164. R.A. Briceño, M.T. Hansen, Phys. Rev. **D94**, 013008 (2016), 1509.08507
165. A. Baroni, R.A. Briceño, M.T. Hansen, F.G. Ortega-Gama (2018), 1812.10504
166. C.W. Andersen, J. Bulava, B. Hörz, C. Morningstar, Phys. Rev. **D97**, 014506 (2018), 1710.01557
167. O. Benhar, N. Farina, H. Nakamura, M. Sakuda, R. Seki, Phys. Rev. **D72**, 053005 (2005), hep-ph/0506116
168. O. Benhar, D. Day, I. Sick, Rev. Mod. Phys. **80**, 189 (2008), nucl-ex/0603029
169. D.G. Middleton, J.R.M. Annand, C. Barbieri, C. Giusti, P. Grabmayr, T. Hehl, I.J.D. MacGregor, I. Martin, J.C. McGeorge, F. Moschini et al., Eur. Phys. J. **A43**, 137 (2010), 0907.1758
170. J. Nieves, F. Sanchez, I. Ruiz Simo, M.J. Vicente Vacas, Phys. Rev. **D85**, 113008 (2012), 1204.5404
171. O. Benhar, P. Huber, C. Mariani, D. Meloni, Phys. Rept. **700**, 1 (2017), 1501.06448
172. N. Rocco, A. Lovato, O. Benhar, Phys. Rev. Lett. **116**, 192501 (2016), 1512.07426
173. N. Rocco, C. Barbieri, Phys. Rev. **C98**, 025501 (2018), 1803.00825
174. S. Dolan, U. Mosel, K. Gallmeister, L. Pickering, S. Bolognesi, Phys. Rev. **C98**, 045502 (2018), 1804.09488
175. O. Benhar, A. Fabrocini, S. Fantoni, Nucl. Phys. **A505**, 267 (1989)
176. O. Benhar, A. Fabrocini, S. Fantoni, Phys. Rev. **C41**, R24 (1990)
177. O. Benhar, A. Fabrocini, S. Fantoni, I. Sick, Nucl. Phys. A **579**, 493 (1994)
178. W.H. Dickhoff, C. Barbieri, Prog. Part. Nucl. Phys. **52**, 377 (2004), nucl-th/0402034
179. K.F. Liu, S.J. Dong, Phys. Rev. Lett. **72**, 1790 (1994), hep-ph/9306299
180. K.F. Liu, S.J. Dong, T. Draper, D. Leinweber, J.H. Sloan, W. Wilcox, R.M. Woloshyn, Phys. Rev. **D59**, 112001 (1999), hep-ph/9806491
181. K.F. Liu, Phys. Rev. **D62**, 074501 (2000), hep-ph/9910306
182. U. Aglietti, M. Ciuchini, G. Corbo, E. Franco, G. Martinelli, L. Silvestrini, Phys. Lett. **B432**, 411 (1998), hep-ph/9804416
183. W. Detmold, C.J.D. Lin, Phys. Rev. **D73**, 014501 (2006), hep-lat/0507007
184. K.F. Liu, PoS **LATTICE2015**, 115 (2016), 1603.07352
185. A.J. Chambers, R. Horsley, Y. Nakamura, H. Perlt, P.E.L. Rakow, G. Schierholz, A. Schiller, K. Somfleth, R.D. Young, J.M. Zanotti (QCDSF), Phys. Rev. Lett. **118**, 242001 (2017), 1703.01153
186. M.T. Hansen, H.B. Meyer, D. Robaina, Phys. Rev. **D96**, 094513 (2017), 1704.08993

187. J. Liang, K.F. Liu, Y.B. Yang, EPJ Web Conf. **175**, 14014 (2018), 1710.11145
188. X. Ji, Phys. Rev. Lett. **110**, 262002 (2013), 1305.1539
189. G. Rossi, M. Testa, Phys. Rev. **D98**, 054028 (2018), 1806.00808
190. K. Cichy, M. Constantinou, Adv. High Energy Phys. **2019**, 3036904 (2019), 1811.07248
191. C. Monahan, PoS **LATTICE2018**, 018 (2018), 1811.00678
192. X. Ji, J.H. Zhang, Y. Zhao, Nucl. Phys. **B924**, 366 (2017), 1706.07416
193. A.V. Radyushkin, Phys. Lett. **B788**, 380 (2019), 1807.07509
194. J. Karpie, K. Orginos, S. Zafeiropoulos, JHEP **11**, 178 (2018), 1807.10933
195. H.W. Lin, J.W. Chen, S.D. Cohen, X. Ji, Phys. Rev. **D91**, 054510 (2015), 1402.1462
196. A.V. Radyushkin, Phys. Rev. **D96**, 034025 (2017), 1705.01488
197. K. Orginos, A. Radyushkin, J. Karpie, S. Zafeiropoulos, Phys. Rev. **D96**, 094503 (2017), 1706.05373
198. Y.Q. Ma, J.W. Qiu, Phys. Rev. Lett. **120**, 022003 (2018), 1709.03018
199. R.S. Sufian, J. Karpie, C. Egerer, K. Orginos, J.W. Qiu, D.G. Richards, Phys. Rev. **D99**, 074507 (2019), 1901.03921
200. J.W. Chen, L. Jin, H.W. Lin, Y.S. Liu, A. Schäfer, Y.B. Yang, J.H. Zhang, Y. Zhao (LP^3) (2018), 1804.01483
201. R.A. Briceño, J.V. Guerrero, M.T. Hansen, C.J. Monahan, Phys. Rev. **D98**, 014511 (2018), 1805.01034
202. G.S. Bali, B. Lang, B.U. Musch, A. Schäfer, Phys. Rev. **D93**, 094515 (2016), 1602.05525
203. J. Karpie, K. Orginos, A. Rothkopf, S. Zafeiropoulos, JHEP **04**, 057 (2019), 1901.05408
204. B. Buck, S.M. Perez, Phys. Rev. Lett. **50**, 1975 (1983)
205. D. Krofcheck et al., Phys. Rev. Lett. **55**, 1051 (1985)
206. W.T. Chou, E.K. Warburton, B.A. Brown, Phys. Rev. **C47**, 163 (1993)
207. A. Baroni, L. Girlanda, S. Pastore, R. Schiavilla, M. Viviani, Phys. Rev. **C93**, 015501 (2016), [Erratum: Phys. Rev.C95,no.5,059901(2017)], 1509.07039
208. H. Krebs, E. Epelbaum, U.G. Meißner, Ann. Phys. **378**, 317 (2017), 1610.03569
209. S. Pastore, A. Baroni, J. Carlson, S. Gandolfi, S.C. Pieper, R. Schiavilla, R.B. Wiringa, Phys. Rev. **C97**, 022501 (2018), 1709.03592
210. A. Lovato, S. Gandolfi, J. Carlson, S.C. Pieper, R. Schiavilla, Phys. Rev. **C91**, 062501 (2015), 1501.01981
211. A. Lovato, S. Gandolfi, J. Carlson, E. Lusk, S.C. Pieper, R. Schiavilla, Phys. Rev. **C97**, 022502 (2018), 1711.02047
212. M.J. Savage, P.E. Shanahan, B.C. Tiburzi, M.L. Wagman, F. Winter, S.R. Beane, E. Chang, Z. Davoudi, W. Detmold, K. Orginos (NPLQCD), Phys. Rev. Lett. **119**, 062002 (2017), 1610.04545
213. E. Chang, Z. Davoudi, W. Detmold, A.S. Gambhir, K. Orginos, M.J. Savage, P.E. Shanahan, M.L. Wagman, F. Winter (NPLQCD), Phys. Rev. Lett. **120**, 152002 (2018), 1712.03221
214. B.C. Tiburzi, M.L. Wagman, F. Winter, E. Chang, Z. Davoudi, W. Detmold, K. Orginos, M.J. Savage, P.E. Shanahan, Phys. Rev. **D96**, 054505 (2017), 1702.02929
215. N. Barnea, L. Contessi, D. Gazit, F. Pederiva, U. van Kolck, Phys. Rev. Lett. **114**, 052501 (2015), 1311.4966
216. A. Bansal, S. Binder, A. Ekström, G. Hagen, G.R. Jansen, T. Papenbrock, Phys. Rev. **C98**, 054301 (2018), 1712.10246
217. L. Contessi, A. Lovato, F. Pederiva, A. Roggero, J. Kirscher, U. van Kolck, Phys. Lett. **B772**, 839 (2017), 1701.06516
218. J. Kirscher, E. Pazy, J. Drachman, N. Barnea, Phys. Rev. **C96**, 024001 (2017), 1702.07268
219. A. Roggero, J. Carlson (2018), 1804.01505
220. W. Detmold, M.G. Endres, Phys. Rev. **D90**, 034503 (2014), 1404.6816
221. S.R. Beane, W. Detmold, K. Orginos, M.J. Savage, J. Phys. **G42**, 034022 (2015), 1410.2937
222. M.L. Wagman, M.J. Savage (2017), 1704.07356
223. M.L. Wagman, M.J. Savage, Phys. Rev. **D96**, 114508 (2017), 1611.07643
224. W. Detmold, G. Kanwar, M.L. Wagman, Phys. Rev. **D98**, 074511 (2018), 1806.01832